

# Large Enhancement of Dye Sensitized Solar Cell Efficiency by Co-sensitizing Pyridyl- and Carboxylic Acid-Based Dyes

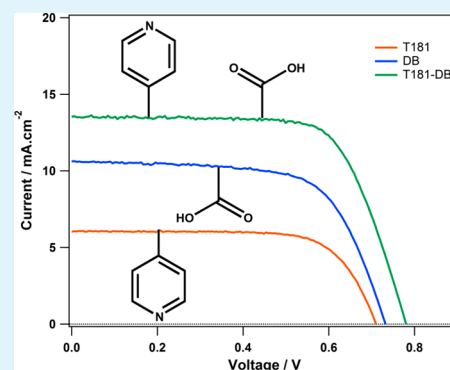
Hamsa M. Hilal, Melissa A. El Bitar Nehme, and Tarek H. Ghaddar\*

Department of Chemistry, American University of Beirut, Beirut 11-0236, Lebanon

## Supporting Information

**ABSTRACT:** Co-sensitization is an attractive approach to enhance the light-harvesting efficiency of a dye sensitized solar cell (DSSC), whereby two or more dyes having complementary absorption spectra are co-adsorbed within a DSSC. A new method of co-sensitizing simultaneously pyridyl- and carboxylic acid-based dyes was performed and proved to be a successful approach for increasing the photoconversion efficiency (PCE%) of a DSSC. Yellow and red pyridyl-based dyes (T181 and T202) were co-sensitized with a blue carboxylic acid-based dye (Dyename Blue, DB). The co-sensitized DSSCs showed profound performance enhancements with a cobalt tris(bipyridine) electrolyte system. Increases in the total cell efficiency of 45% and 16% were seen in the co-sensitized T181-DB and T202-DB cells when compared to the single dye-sensitized DB cell, respectively. Remarkable increases in photocurrent ( $J_{sc}$ ) and photovoltage ( $V_{oc}$ ) were seen in both co-sensitized cells. The higher  $V_{oc}$  values were mainly due to the decrease in the electron recombination processes at the  $TiO_2$ /cobalt electrolyte interface. The increase in dye coverage in the co-sensitized cells resulted in a blocking behavior at the  $TiO_2$ /electrolyte interface and had positive effects on electron lifetime. In addition the higher  $J_{sc}$  values were associated with the complementary absorption responses of T181 and T202 with DB as mirrored in the IPCE% spectra.

**KEYWORDS:** DSSC, impedance spectroscopy, cobalt electrolyte, pyridine dyes, solar cells, co-adsorption, co-sensitization



## INTRODUCTION

Since the pioneer work of Grätzel and O'Regan on dye-sensitized solar cells (DSSCs) in 1991,<sup>1</sup> immense research in this area has been mainly demonstrated on increasing the DSSC efficiency. Thousands of different dye sensitizers have been molecularly engineered and employed in DSSCs with different electrolyte systems where efficiencies approaching 15% have been attained.<sup>2–4</sup> Recently, renewed interest in the DSSC field has re-emerged due to the device's attractive aesthetic properties<sup>5</sup> and superior functionality at low-light conditions that make it attractive for indoor applications.<sup>6,7</sup>

One of the successful attempts to enhance the light-harvesting efficiency of a DSSC is co-sensitization, whereby two dyes having complementary absorption spectra are co-sensitized together within the solar cell.<sup>2,8–11</sup> This method would generally result in higher photocurrents and a “maximized” IPCE% in the absorption regions of both dyes. However, most of the commonly used dyes for co-sensitization contain a carboxylic acid anchoring group since it facilitates electron injection from the dye to the metal oxide semiconductor by binding to  $TiO_2$  by a firm monodentate ester, bidentate chelating, bidentate bridging, and monodentate and bidentate H-bonding, as well as monodentate coordinating mode linkage.<sup>12</sup> It is well-known that carboxylic acid binds to the Brønsted acid sites ( $TiOH$ ) of  $TiO_2$  that comprise ~50–60% of the total number of adsorption sites in titania.<sup>13</sup> On the other hand, the rest of the sites (~40–50%), considered to be

Lewis acid sites ( $Ti^{+n}$ ), are mostly free and usually “shielded” by an additive (such as the commonly used additives *t*-butylpyridine or benzimidazole) that adsorbs onto these sites in a fully operational DSSC.<sup>14</sup> As such, the co-sensitization of dyes having carboxylic acid anchoring groups would often lead to a decrease in the amounts of both adsorbed dyes when compared to adsorbing each dye alone within a DSSC.<sup>9,10,15</sup> This decrease in the total dyes' loading is due to the competitive adsorption of both dyes on the same Brønsted acid sites of  $TiO_2$ .

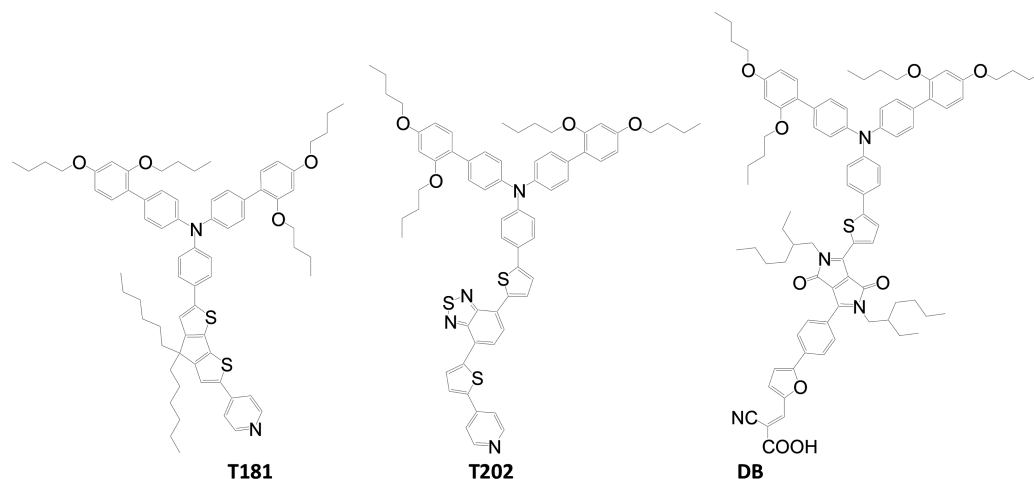
In 2011, Harima et al. reported on new efficient dyes having a pyridyl moiety as an anchoring group,<sup>16,17</sup> and it was proven by the same group later in 2013 that such dyes adsorb preferentially on the Lewis acid sites of  $TiO_2$ .<sup>13</sup> Moreover, in the same latter study, co-adsorbing either the NI2 dye having a carboxylic acid anchoring group or the pyridine-based NI4 dye with 4-carboxy TEMPO (4CT) showed that, under the co-adsorption conditions, the Brønsted acid sites are occupied by 4CT, preventing the adsorption of NI2 on the same sites. However, 4CT had no effect on the amount of adsorbed NI4 since the latter adsorbs preferentially at the Lewis acid sites. In 2014, Arakawa and co-workers presented an increase in the short-circuit current ( $J_{sc}$ ) of DSSCs co-sensitized with the Black

Received: March 20, 2018

Accepted: May 14, 2018

Published: May 14, 2018

Scheme 1. Molecular Structures of T181, T202, and DB Dyes



dye and a pyridine-anchor organic dye. The higher  $J_{sc}$  was caused by the increase in light absorption in the blue region of the spectrum where the pyridine-based dye absorbs.<sup>18,19</sup>

Inspired by the fact that pyridine binds largely to the Lewis acid sites whereas the carboxylic acid binds to the Brønsted acid sites of  $\text{TiO}_2$ , we designed and synthesized two new pyridine-based dyes (T181 and T202) and studied their co-sensitization with a commercially available blue dye (Dyename Blue, DB<sup>9</sup>) that contains a carboxy anchoring group, Scheme 1. The selection of co-sensitizing T181 or T202 with DB was mainly based on their complementary absorption spectra, where both T181 and T202 absorb in the region where DB has its lowest absorption. In addition, T181 and T202 were engineered with a large donor group that proved to be very beneficial with cobalt-based electrolyte systems, especially in decreasing charge recombination in a DSSC.<sup>20</sup> Such an approach shall contribute to an increase in the total dye loading amount while conserving the loading amount of the carboxylic acid-based dyes resulting in higher  $J_{sc}$  values. In addition, the high surface coverage of  $\text{TiO}_2$  achieved by using this co-sensitization strategy with the new dyes could result in positive effects on the open-circuit voltage ( $V_{oc}$ ) due to blockage of electron-recombination pathways from the titania to the cobalt electrolyte system.

## EXPERIMENTAL SECTION

**Materials and Instrumentation.** All organic chemicals were purchased from Sigma-Aldrich and used as supplied. The Dyename Blue dye and 2',4'-dibutoxy-*N*-(2',4'-dibutoxy-[1,1'-biphenyl]-4-yl)-*N*-(4-(4,4,5,5-tetramethyl-1,3,2-dioxaborolan-2-yl)phenyl)-[1,1'-biphenyl]-4-amine were purchased from Dyename (Sweden). FTO glass "Tec15" and "Tec8" were purchased from Pilkington (USA).  $\text{TiO}_2$  colloids 30NR-D and WER2-O were purchased from Dyesol (Australia). 2,6-Dibromo-4,4-dihexyl-4*H*-cyclopenta[2,1-*b*:3,4-*b'*]-dithiophene<sup>21</sup> and 4,7-bis(5-bromo-2-thienyl)-2,1,3-benzothiadiazole<sup>22</sup> were prepared according to reported procedures in the literature. The NMR spectra ( $^1\text{H}$  and  $^{13}\text{C}$ ) were measured on a Bruker AM 500 MHz spectrometer. UV-vis spectra were recorded on a Jasco V-570 UV-vis-near-IR spectrometer. Steady state emission spectra were measured on a JobinYvon Horiba Fluorolog-3 spectrofluorometer. The electrochemical setup consisted of a three-electrode cell, with a platinum rod as the working electrode, a Pt wire  $\sim 1$  mm diameter as the counter electrode, and  $\text{Ag}/\text{Ag}^+$  (10 mM  $\text{AgNO}_3$ ) as the reference electrode. The electrochemical measurements were performed in 0.1  $\text{LiClO}_4$  in DMF, and  $\text{Fc}/\text{Fc}^+$  standard (0.69 vs NHE in DMF) was used as an internal reference. Electrochemical impedance spectra of the DSSCs were performed with CH Instruments 760B (USA). The

obtained impedance spectra were fitted with the Z-view software (v2.8b, Scribner Associates Inc.). The spectra were performed in the frequency range 0.1– $10^5$  Hz with oscillation potential amplitudes of 10 mV at RT under open-circuit conditions at different light levels. IPCE% spectra were recorded using a Newport 74000 Cornerstone monochromator. Photocurrent vs voltage characteristics were measured with a Keithley 2400 source meter and a solar simulator illuminated by a Xenon arc lamp (Oriel) through an AM1.5 simulation filter (ScienceTech). The irradiated area of the cell was  $0.5 \times 0.5 \text{ cm}^2$  with a  $0.6 \times 0.6 \text{ cm}^2$  black mask.

**Computational Methods.** Calculations were carried out using Gaussian 03.<sup>23</sup> Geometries were optimized using the 6-31G\* basis set with (B3LYP) in water (C-PCM algorithm).<sup>24</sup>

**Solar Cell Fabrication.** Dye-sensitized solar cells were fabricated using standard procedures. A compact titania layer (Ti-nanoxide BL/SP, Solaronix, Switzerland) was first spin-coated on a cleaned "Tec15" conductive glass, followed by treatment with 40 mM  $\text{TiCl}_4$  aqueous solution at 70 °C for 30 min. A 4  $\mu\text{m}$  titania layer was then printed by the doctor blading method from a diluted  $\text{TiO}_2$  paste (60%  $\text{TiO}_2$  Dyesol 30NR-D, 34% terpineol and 6% ethyl cellulose), followed by a scattering layer (4  $\mu\text{m}$ ) of Dyesol WER2-O  $\text{TiO}_2$  paste. Next, the electrodes were sintered at 500 °C for 60 min, followed by treatment with 40 mM  $\text{TiCl}_4$  aqueous solution at 70 °C for 30 min. The films were further heated at 500 °C for 60 min before sensitizing with 0.2 mM T181/T202 and/or with 0.03 mM DB in 1:1:1 THF/acetonitrile/*tert*-butanol mixture. The counter electrodes were fabricated by applying a 2–3  $\mu\text{L}/\text{cm}^2$  of 5 mM  $\text{H}_2\text{PtCl}_6$  in 2-propanol to the "Tec8" FTO glass, followed by heating in an oven at 400 °C for 20 min. Cell assembly was performed by sealing the counter electrode to the  $\text{TiO}_2$  electrode with a 25  $\mu\text{m}$  Surlyn (Dupont) spacer at  $\sim 100$  °C for 3 min. The cobalt electrolyte (the electrolyte consisted of 0.25 M  $\text{Co}^{\text{II}}(\text{bpy})_2 \cdot 2\text{PF}_6$ , 0.06 M  $\text{Co}^{\text{III}}(\text{bpy})_2 \cdot 3\text{PF}_6$ , 0.1 M  $\text{LiClO}_4$ , and 0.2 M *t*-butylpyridine (TBP) in acetonitrile) was introduced through two small holes, previously drilled through the counter electrode, which were then sealed with Surlyn.

**Preparation of T181.** In an argon-degassed medium of 5:1:1 dioxane:tetrahydrofuran:water, a mixture of 2,6-dibromo-4,4-dihexyl-4*H*-cyclopenta[2,1-*b*:3,4-*b'*]dithiophene<sup>21</sup> (0.4 g, 0.6 mmol), 4-pyridinylboronic acid (0.09 g, 0.73 mmol), 2',4'-dibutoxy-*N*-(2',4'-dibutoxy-[1,1'-biphenyl]-4-yl)-*N*-(4-(4,4,5,5-tetramethyl-1,3,2-dioxaborolan-2-yl)phenyl)-[1,1'-biphenyl]-4-amine (0.58 g, 0.72 mmol), triphenylphosphine (0.08 g, 0.29 mmol), potassium carbonate (1.35 g, 9.77 mmol), and palladium acetate (12 mg, 0.05 mmol) was stirred under reflux for 48 h. The product was extracted into dichloromethane and washed with water. Then, the organic layer was dried over anhydrous potassium carbonate and filtered and the solvent was removed under reduced pressure. The product was purified by column chromatography on silica gel with hexane:ethyl acetate as the eluting solvent, and the main band was collected. Finally, the solvent was

removed under reduced pressure to get an orange compound (142 mg, 21% yield).  $^1\text{H NMR}$  (500 MHz, acetone- $d_6$ ):  $\delta$  8.41 (dd,  $J_1 = 4.5$  and  $J_2 = 1.6$  Hz, 2H), 7.71 (s, 1H), 7.53 (d,  $J = 8.7$  Hz, 2H), 7.48 (dd,  $J_1 = 4.5$  and  $J_2 = 1.6$  Hz, 2H), 7.40 (d,  $J = 8.7$  Hz, 4H), 7.38 (s, 1H), 7.16 (d,  $J = 8.4$  Hz, 2H), 7.03 (d,  $J = 2.1$  Hz, 3H), 7.03 (d,  $J = 8.7$ , 6.6 Hz, 3H), 6.53 (d,  $J = 2.4$  Hz, 2H), 6.48 (dd,  $J_1 = 8.4$  and  $J_2 = 2.4$  Hz, 2H), 3.92 (t, 4H), 3.92 (t, 4H), 1.63 (quint, 4H), 1.63 (quint, 4H), 1.37 (sixt, 4H), 1.37 (sext, 4H), 1.20–1.00 (m, 10H), 0.84 (t, 6H), 0.67 (t, 6H).  $^{13}\text{C NMR}$  (126 MHz, acetone):  $\delta$  160.40, 159.90, 158.79, 157.09, 150.38, 147.37, 146.02, 145.49, 141.92, 140.44, 138.66, 134.28, 133.81, 130.64, 130.30, 128.89, 126.00, 123.71, 123.55, 122.56, 120.70, 118.58, 117.36, 105.84, 100.24, 67.88, 67.42, 54.33, 37.62, 31.45, 31.27, 31.15, 24.36, 22.36, 19.16, 19.05, 13.38, 13.25. APPI MS ( $m/z$ ): calcd for  $\text{C}_{72}\text{H}_{86}\text{N}_2\text{O}_4\text{S}_2$  [ $\text{M} + \text{H}^+$ ] $^+$ , 1107.6; found, 1108.1.

**Preparation of T202.** In a 50 mL round-bottom flask, 4,7-bis(5-bromo-2-thienyl)-2,1,3-benzothiadiazole<sup>22</sup> (0.15 g, 0.33 mmol), 4-pyridinyl boronic acid (44 mg, 0.36 mmol), and 2',4'-dibutoxy-N-(2',4'-dibutoxy-[1,1'-biphenyl]-4-yl)-N-(4-(4,4,5,5-tetramethyl-1,3,2-dioxaborolan-2-yl)phenyl)-[1,1'-biphenyl]-4-amine (0.30 g, 0.36 mmol) were mixed along with triphenylphosphine (40 mg, 0.144 mmol), potassium carbonate  $\text{K}_2\text{CO}_3$  (0.67 g, 4.85 mmol), and palladium acetate  $\text{Pd}(\text{OAc})_2$  (5.6 mg, 0.025 mmol). A 25 mL of 3:2:1 dioxane:THF:water was added, and the solution was purged with argon and refluxed for 48 h. The solvent was then removed under reduced pressure, and the dark red solid was then dissolved in dichloromethane, washed with water, and dried with sodium sulfate. The resulting compound was purified by column chromatography on silica gel with a gradient elution of dichloromethane and methanol. T202 was isolated as a purple compound (at 1% methanol in dichloromethane) (120 mg, 34.6% yield).  $^1\text{H NMR}$  (500 MHz, benzene- $d_6$ ):  $\delta$  8.55 (d,  $J = 5.0$  Hz, 2H), 8.25 (d,  $J = 3.9$  Hz, 1H), 8.03 (d,  $J = 3.9$  Hz, 1H), 7.70–7.65 (m, 4H), 7.58–7.54 (m, 2H), 7.51 (d,  $J = 7.7$  Hz, 1H), 7.38 (d,  $J = 8.4$  Hz, 2H), 7.32 (dd,  $J_1 = 2.3$  and  $J_2 = 9.0$  Hz, 5H), 7.24 (d,  $J = 2.1$  Hz, 1H), 7.23–7.21 (m, 2H), 7.19 (d,  $J = 3.9$  Hz, 2H), 6.99 (q,  $J = 1.2$  Hz, 1H), 6.67 (d,  $J = 2.4$  Hz, 2H), 6.53 (dd,  $J_1 = 2.4$  and  $J_2 = 8.5$  Hz, 2H), 3.75 (t,  $J = 6.4$  Hz, 4H), 3.64 (t,  $J = 6.4$  Hz, 4H), 1.67–1.62 (m, 4H), 1.52–1.47 (m, 4H), 1.44–1.39 (m, 4H), 1.30–1.25 (m, 4H), 0.90–0.86 (m, 8H), 0.79 (s, 4H).  $^{13}\text{C NMR}$  (126 MHz, benzene- $d_6$ ):  $\delta$  160.57, 157.87, 153.03, 151.22, 148.67, 146.70, 146.43, 142.43, 141.66, 141.14, 138.28, 134.74, 131.64, 131.25, 130.17, 127.35, 126.54, 126.13, 125.24, 125.08, 124.78, 124.32, 123.97, 123.95, 119.88, 105.87, 101.40, 68.28, 67.90, 31.95, 31.66, 19.83, 19.81, 14.23, 14.17. MALDI-TOF MS ( $m/z$ ): calcd for  $\text{C}_{65}\text{H}_{64}\text{N}_4\text{O}_4\text{S}_3$ , 1061.4; found, 1061.3.

## RESULTS AND DISCUSSION

The yellow and red dyes, T181 and T202, respectively, were synthesized as in the general synthetic route shown in Scheme S1 (Supporting Information). The middle linker parts were combined to the triphenylamine donor moiety and the pyridine anchoring group simultaneously by a Suzuki coupling reaction. The characterizations of the two new dyes and details of synthesis are described in the Experimental Section.

The absorption and emission spectra of T181 and T202 are shown in Figure 1. The absorption maxima of T181 and T202 were exhibited at 442 and 520 nm with molar absorptivities ( $\epsilon$ ) of  $3.8 \times 10^4$  and  $4.3 \times 10^4 \text{ M}^{-1} \text{ cm}^{-1}$ , respectively. The emission maxima in THF are at 570 and 705 nm with quantum yields of 0.75 and  $\leq 0.05$  for T181 and T202, respectively. The derived redox potentials of the dyes' excited states from both the redox potential (Figure S1 in the Supporting Information) and the optical energy gap ( $E_{0-0}$  was calculated from the intersection of the lowest energy absorption and emission bands) were found to be ( $E_{(\text{ox})} - E_{0-0}$ ) =  $-1.46$  and  $-1.08$  V vs NHE for T181 and T202, respectively. These values are higher than that of the  $\text{TiO}_2$  conduction band edge (CB) ( $-0.5$  V vs NHE), and thus upon photoexcitation of both dyes, fast and

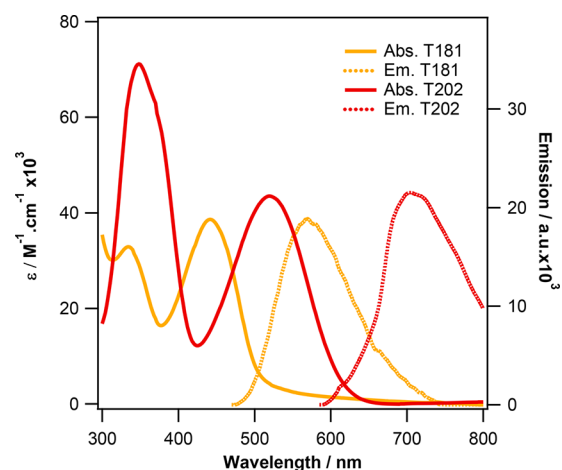


**Figure 1.** Absorption (solid) and emission (dotted) spectra of T181 and T202 in THF ( $\lambda_{\text{ex}} = 450$  and 550 nm for T181 and T202, respectively).

efficient electron injection into the  $\text{TiO}_2$  CB is expected. The photophysical and electrochemical details of the two dyes including that of DB can be found in Table 1.

**Table 1. Photophysical and Electrochemical Properties of T181, T202, and the DB Dye**

dye	abs ( $\epsilon \times 10^4 \text{ M}^{-1} \text{ cm}^{-1}$ )	$\lambda_{\text{em}}$ , nm ( $\phi_f$ )	$E_{\text{ox}}$ , V vs NHE	$E_{\text{ox}} - E_{0-0}$ , V vs NHE
T181	336 (3.3), 442 (3.8) <sup>a</sup>	570 (0.75) <sup>a</sup>	1.00 <sup>b</sup>	-1.46
T202	350 (7.1), 520 (4.3) <sup>a</sup>	705 ( $\leq 0.05$ ) <sup>a</sup>	1.05 <sup>b</sup>	-1.08
DB <sup>c</sup>	340 (4.5), 577 (3.4)	725 (N.R.)	1.08	-0.87

<sup>a</sup>Absorption and emission spectra were measured in THF at 25 °C;  $\lambda_{\text{ex}} = 500$  and 600 nm for T181 and T202, respectively. <sup>b</sup>The redox potentials were measured in DMF containing 0.1 M (TBA)PF<sub>6</sub> as supporting electrolyte, a platinum working electrode, and an Ag/Ag<sup>+</sup> (calibrated with ferrocene/ferrocenium as an internal standard) reference electrode. <sup>c</sup>Data from ref 9.

In order to check the effect of co-sensitizing the pyridyl-based dyes (T181 and T202) with the carboxylic acid-based dye (DB) on the individual and total dyes' loading, we performed absorbance measurements on sensitized and co-sensitized films in addition to the corresponding desorbed solutions. Figure 2 shows the absorbance spectra of  $\text{TiO}_2$  films sensitized individually with each dye, in addition to the two co-sensitized films (T181 plus DB denoted as T181-DB, and T202 and DB denoted as T202-DB). As can be deduced from Figure 2, the two co-sensitized films appeared to be very different, i.e., different amounts of DB present in both films. In order to measure the actual dyes' loadings in all of the sensitized films, they were desorbed in 0.01 M KOH in 1:9 water:THF followed by measuring the corresponding solutions' absorbance spectra (Figures S2 and S3) and spectra fitting of the desorbed solutions from the co-sensitized films. The dye desorption measurements data are found in Table 2. The dye loading measurement of the co-sensitized T181-DB film (29.2 nmol·cm<sup>-2</sup> of DB and 21.0 nmol·cm<sup>-2</sup> of T181) shows clearly that both dyes (T181 and DB) do not compete for adsorption sites on  $\text{TiO}_2$ , since as predicted, the T181 dye preferentially adsorbs onto the Lewis acid sites whereas the DB dye adsorbs onto to the Brønsted acid sites of  $\text{TiO}_2$ . However, the striking

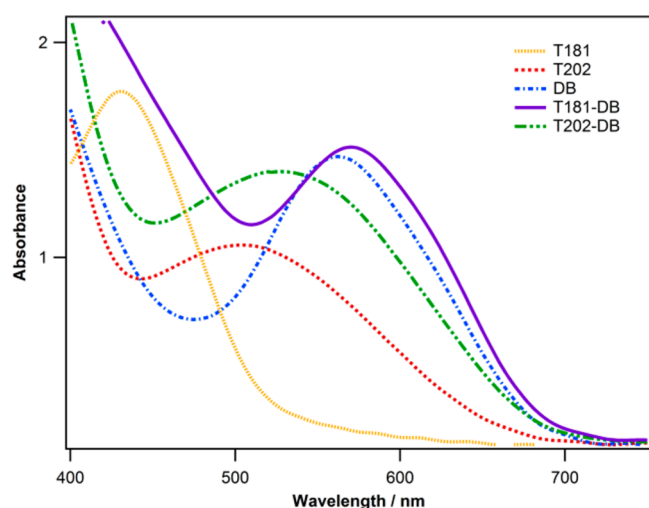


**Figure 2.** UV-vis spectra of T181, T182, DB, and co-sensitized T181-DB and T202-DB dyes on 4  $\mu\text{m}$   $\text{TiO}_2$  films.

**Table 2.** Dye-Loadings Measurements of Single-Dye-Sensitized- and Co-sensitized  $\text{TiO}_2$  Films<sup>a</sup>

film	dye loading ( $\text{nmol cm}^{-2}$ )	total dye loading ( $\text{nmol cm}^{-2}$ )
DB	$29.0 \pm 0.3$	$29.0 \pm 0.3$
T181	$21.0 \pm 0.1$	$21.0 \pm 0.1$
T202	$27.8 \pm 0.2$	$27.8 \pm 0.2$
T181-DB	$21.0 \pm 0.1$ (T181), $29.2 \pm 0.3$ (DB)	$50.2 \pm 0.4$
T202-DB	$29.4 \pm 0.2$ (T202), $10.1 \pm 0.3$ (DB)	$39.5 \pm 0.5$

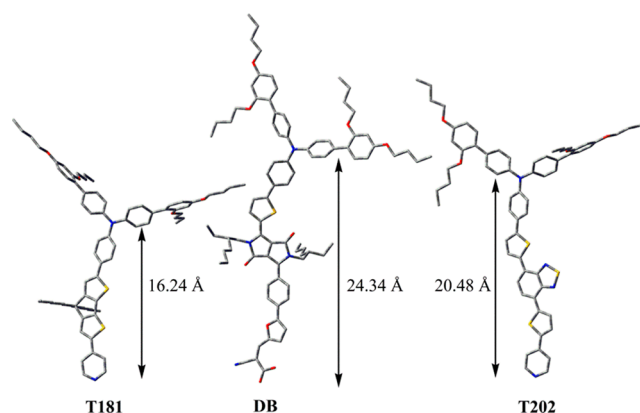
<sup>a</sup>A 4  $\mu\text{m}$   $\text{TiO}_2$  film of  $1.6 \times 1.6 \text{ cm}^2$  was used. The dye bath concentrations were 0.2 mM for T181 and T202 and 0.03 mM for DB. Each measurement was done in duplicate.

difference was seen in the T202-DB co-sensitized film, where the T202 loading ( $29.4 \text{ nmol}\cdot\text{cm}^{-2}$ ) was similar to the single dye-sensitized T202 film ( $27.8 \text{ nmol}\cdot\text{cm}^{-2}$ ), but the amount of adsorbed DB dye in the T202-DB film ( $10.1 \text{ nmol}\cdot\text{cm}^{-2}$ ) was  $\sim 65\%$  less than the single dye-sensitized DB film ( $29.0 \text{ nmol}\cdot\text{cm}^{-2}$ ). This result explains the differences seen between the two absorption spectra of the co-sensitized films in Figure 1. In addition, the extinction coefficients of the adsorbed T181 and T202 ( $\epsilon_f$ ) at their absorption maxima were calculated and found to be  $5.7 \times 10^4$  and  $3.8 \times 10^4 \text{ M}^{-1}\cdot\text{cm}^{-1}$ , respectively. The lower  $\epsilon_f$  value of T202 is most probably due to its broadened absorption when adsorbed to  $\text{TiO}_2$ .<sup>25</sup> The broadening of T202 absorption when adsorbed on  $\text{TiO}_2$  can be clearly seen when comparing its absorption spectra in solution and on film in Figures 1 and 2, respectively. However, the striking finding is the higher  $\epsilon_f$  value of T181 than that in solution. Interestingly and unlike the T202 case, no significant broadening of adsorbed T181's absorption band was seen (Figure S4 in Supporting Information), which in turn would not lower its  $\epsilon_f$  value. In addition, we speculate that upon  $\text{TiO}_2$  sensitization with T181 a new electronic transition might arise (between T181 and  $\text{TiO}_2$ ) which overlaps with T181's lowest energy electronic transition and hence this might be the reason behind the increase of the  $\epsilon_f$  value of T181 on  $\text{TiO}_2$ .

In general, one of the important factors that usually researchers pay attention to when co-sensitizing carboxylic acid-based dyes is the matching of the dyes' structural sizes.<sup>26</sup>

With this in mind we performed density functional theory (DFT) calculations on the three dyes. Scheme 2 shows the

**Scheme 2.** Calculated Relative Sizes of the Geometry Optimized T181, T202, and DB Dyes



relative sizes of the dyes. The calculated vertical distances between the N atom of the triphenylamine donor moiety to the N atom of the pyridyl moiety are 16.24 and 20.48 Å for T181 and T202, respectively, whereas the distance between the triphenylamine N atom and the O atom of the carboxylic acid moiety in the DB dye is 24.34 Å. As can be seen in Scheme 2, the bulky donor group of T181 can fit within the groove right below the DB's triphenylamine donor group; however, this is not the case in T202. Therefore, we speculate that the reason behind the lower loading of DB in the T202-DB co-sensitized film might be only due to a complementary size relationship between the co-sensitized dyes, where T181 has a more suitable shape and size than T202 which make the former dye fit better within the voids of the adsorbed DB dye molecules. It is important to note here that we did not increase the DB concentration in the T202-DB film bath above 0.03 mM to increase its loading amount mainly because the DB is very prone to aggregation,<sup>27</sup> and therefore any higher concentration would greatly and negatively affect our DSSC efficiency measurements. Based on the above results it is suggested that site selective adsorption was achieved when co-sensitizing T181 or T202 with DB.

Liquid DSSCs were fabricated to test the photovoltaic performance upon co-sensitizing T181 and T202 with DB, Figures 3 and 4. The output characteristics are summarized in Table 3. The DB-based DSSC had a power conversion efficiency (PCE) of 5.1%, which is higher than that of T181 and T202 that showed PCEs of 3.1 and 4.7%, respectively. Interestingly, the T202-based cell showed a bit higher  $J_{sc}$  and similar  $V_{oc}$  ( $J_{sc} = 11.1 \text{ mA}\cdot\text{cm}^{-2}$  and  $V_{oc} = 739 \text{ mV}$ ) to those of DB ( $J_{sc} = 10.6 \text{ mA}\cdot\text{cm}^{-2}$  and  $V_{oc} = 737 \text{ mV}$ ). This finding shows that T202 is a very efficient pyridyl-based dye; however, T181 showed a lower  $J_{sc} = 6.1 \text{ mA}\cdot\text{cm}^{-2}$  than DB that is primarily due to its limited absorption in the visible region as mirrored in the IPCE% spectrum, Figure 3B.

Upon co-sensitizing T181 or T202 with DB, remarkable increases in the PCE%,  $J_{sc}$  and  $V_{oc}$  were seen, Figures 3 and 4 and Table 3. For the T181-DB co-sensitized DSSC a 45% increase in the PCE% (7.4%) was seen when compared to DB alone (PCE% = 5.1%), whereas T202-DB showed a 16% increase in PCE% (6.0%). The  $V_{oc}$  increased by 44 and 53 mV for the two co-sensitized DSSCs when compared to that of DB,

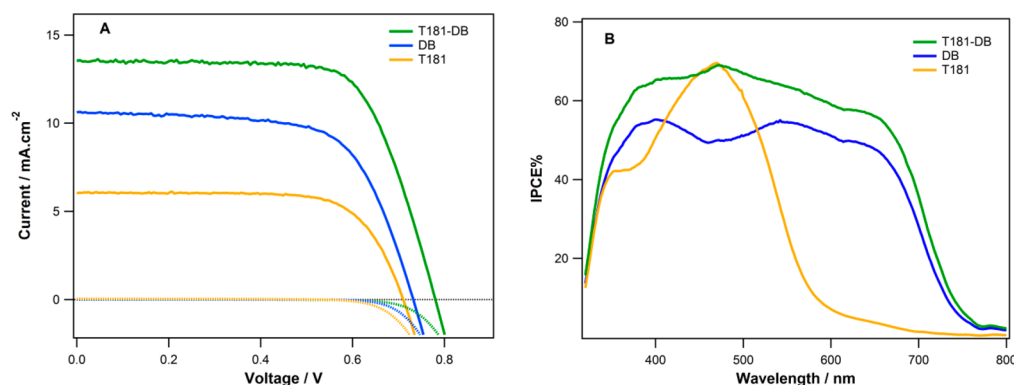


**Figure 3.** (A) Photocurrent–voltage characteristics of DSSCs sensitized with T181, DB, and co-sensitized T181-DB; (B) corresponding IPCE% spectra.

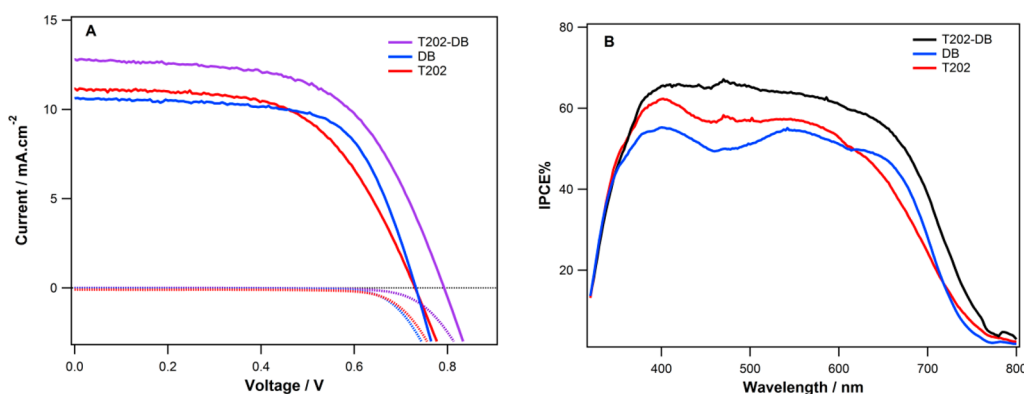


**Figure 4.** (A) Photocurrent–voltage characteristics of DSSCs sensitized with T1202, DB, and co-sensitized T202-DB; (B) corresponding IPCE% spectra.

**Table 3. Photovoltaic Performance of the T181, T202, and DB DSSCs and Co-sensitized Dyes (T181-DB and T202-DB)<sup>a</sup>**

dye	$J_{sc}$ mA cm <sup>-2</sup>	$V_{oc}$ mV	FF	PCE, %
T181	6.1 (6.0) <sup>b</sup>	712	0.71	3.1
T202	11.1 (11.2) <sup>b</sup>	739	0.57	4.7
DB	10.6 (10.7) <sup>b</sup>	737	0.66	5.1
T181-DB	13.3 (13.0) <sup>b</sup>	781	0.71	7.4
T202-DB	12.8 (12.9) <sup>b</sup>	792	0.59	6.0

<sup>a</sup>Measured under 100 mW cm<sup>-2</sup> simulated AM1.5 spectrum with an active area of 0.5 × 0.5 cm<sup>2</sup> and a black mask (0.6 × 0.6 cm<sup>2</sup>); the electrolyte consisted of 0.25 M Co(II), 0.06 M Co(III), 0.1 M LiClO<sub>4</sub> and 0.2 M TBP. <sup>b</sup>Integrated photocurrent (AM1.5 Global).

most probably due to a decrease in electron recombination from the TiO<sub>2</sub> to the cobalt electrolyte as suggested by the dark currents seen in Figures 3 and 4. This decrease in electron recombination could be due to the blocking of the cobalt electrolyte from approaching the titania surface because of the close arrangement of the co-sensitized dyes on the surface. The increase of the  $J_{sc}$  values of both co-sensitized cells ( $J_{sc} = 13.3$  and 12.8 for T181-DB and T202-DB, respectively) is mainly due to the complementary absorption responses of T181 and T202 with the DB dye. This result is also consistent with the IPCE% responses of both co-sensitized DSSCs especially in the 400–600 nm region where T181 and T202 have their maximum absorption.

In order to understand the above-mentioned results (high efficiencies of T181-DB and T202-DB cells), we performed

electrochemical impedance spectroscopy (EIS) measurements on the five different assembled cells at  $V_{oc}$  under different light intensities. Figures 5 and 6 show plots of the chemical capacitance ( $C_{\mu}$ ) and the charge recombination resistance ( $R_{CT}$ ) values at the TiO<sub>2</sub>/electrolyte interface, respectively. For the five DSSCs, the  $R_{CT}$  and  $C_{\mu}$  values were extracted from the EIS experiments vs the applied voltage ( $nE_F - E_{F,redox}$ ), where

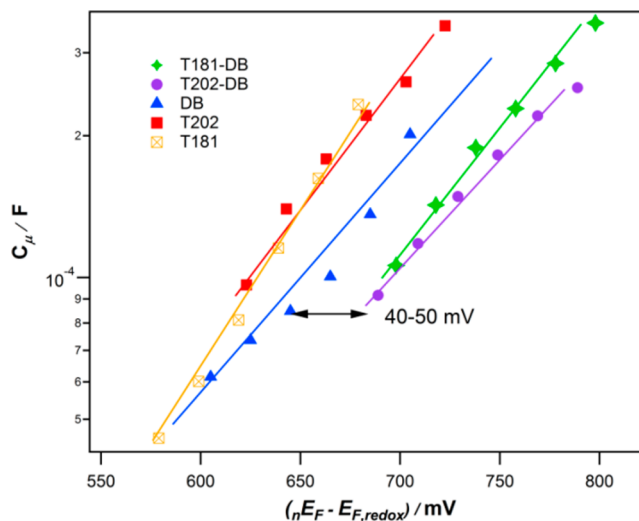


**Figure 5.** Chemical capacitance values obtained from EIS of T181, T202, DB, and co-sensitized T181-DB and T202-DB cells (lines are just eye guides).

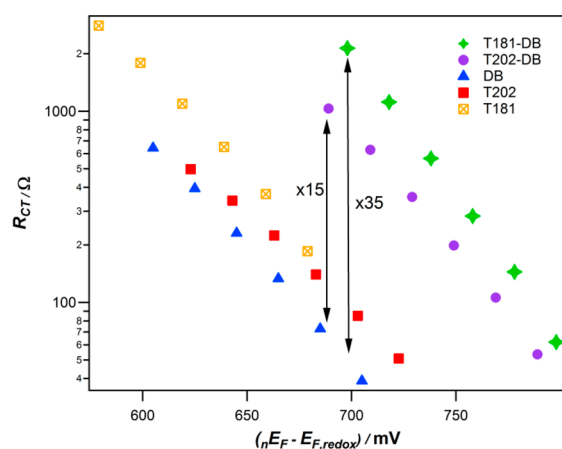


**Figure 6.** Charge transfer resistance values obtained from EIS of T181, T202, DB, and co-sensitized T181-DB and T202-DB cells.

${}_nE_F$  is the electron quasi-Fermi energy level in the  $\text{TiO}_2$  film and  $E_{F,\text{redox}}$  is the electrolyte redox Fermi level. In Figure 5, both T181-DB and T202-DB co-sensitized devices show a shift  $\Delta({}_nE_F - E_{F,\text{redox}})$  of  $\sim 40\text{--}50$  mV higher than the DB device at a certain  $C_\mu$  value. A shift in  $({}_nE_F - E_{F,\text{redox}})$  toward higher or lower values is attributed to an upward or downward shift in the  ${}_nE_F$  with respect to the electrolyte  $E_{F,\text{redox}}$ , respectively, since the same electrolyte composition is used in all DSSCs.<sup>28,29</sup> The upward shift in the  ${}_nE_F$  in the two co-sensitized cells could be one of the reasons behind the higher  $V_{\text{oc}}$  values for these cells. However, this upward shift of  ${}_nE_F$  in the two co-sensitized cells is counterintuitive, since the DB dye contains one carboxylic acid proton that would usually result in a  $\sim 20$  mV downward shift of the conduction band, and one would expect a decrease in the  $V_{\text{oc}}$  values upon co-sensitizing T181 and T202 with DB. Therefore, we speculate that the above-mentioned  $\Delta({}_nE_F - E_{F,\text{redox}})$  shift is rather due to the differences in the total dyes' coverage on  $\text{TiO}_2$ . A lower dye coverage, such as in the case of the DB cell when compared to the co-sensitized T181-DB and T202-DB cells, would result in lower electron injection rates into  $\text{TiO}_2$  and subsequently lead to a lower  ${}_nE_F$  and hence lower  $V_{\text{oc}}$  at 1 sun.<sup>30–32</sup> Boschloo et al. have showed before that the dye loading has pronounced effect on the photovoltage in the case of cobalt electrolyte.<sup>33</sup> In their EIS experiments a similar trend in the  $\Delta({}_nE_F - E_{F,\text{redox}})$  is seen, where a shift to higher values was seen with increasing dye loadings.

In Figure 6, the  $R_{\text{CT}}$  values of the two co-sensitized cells are way higher than that of the DB device (35 and 15 times higher for T181-DB and T202-DB than DB, respectively). Again, higher  $R_{\text{CT}}$  values and thus lower electron recombination in the T181-DB and T202-DB are probably due to the blockage of the electrolyte pathway to the titania and hence less electron recombination processes; in a way similar to the effect of dye loading on the cell efficiency seen by Booschlo et al.<sup>33</sup> Therefore, the upward shift in the  ${}_nE_F$  and the higher charge recombination resistances in the two co-sensitized solar cells well-explain their higher cell efficiencies when compared to the DB one. The electron lifetime ( $\tau_n$ ) in all solar cells was evaluated from the EIS experiments ( $\tau_n = R_{\text{CT}}C_\mu$ ) and is shown in Figure 7. The  $\tau_n$  values are consistent with the slower recombination processes in the T181-DB and T202-DB co-sensitized solar cells when compared to DB.

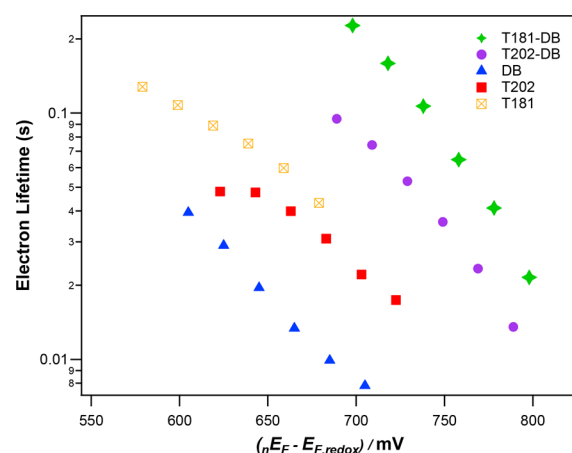


**Figure 7.** Electron lifetime values obtained from EIS of T181, T202, DB, and co-sensitized T181-DB and T202-DB cells.

## CONCLUSIONS

In summary, we were successful to synthesize two pyridyl-based dyes (T181 and T202) and co-sensitize them with a carboxylic acid-based one (Dyename Blue, DB) in fully operating DSSCs using a cobalt-based electrolyte system. The dye loading measurements of the co-sensitized T181-DB film clearly demonstrated that both dyes do not compete for the same adsorption sites on  $\text{TiO}_2$ , and therefore the total dye loading was about the sum of the amounts of the two dyes as in the single dye-sensitized films. However, the dye loading measurements of the co-sensitized T202-DB film showed a surprisingly different result, which was explained by the complementary size relationship between the dyes, where T202, in contrary to T181, does not possess a suitable size and shape to fit appropriately the voids within the adsorbed DB dye molecules on the titania film. Moreover, the photovoltaic performances of liquid DSSCs co-sensitized with T181-DB and T202-DB were enhanced in comparison to a DSSC sensitized with DB alone. The co-sensitized DSSCs showed higher open-circuit voltages explained by the decrease of the electron recombination between  $\text{TiO}_2$  and the cobalt electrolyte by preventing it from approaching the packed surface on  $\text{TiO}_2$ , in addition to higher short-circuit currents associated with the complementary absorption responses of T181 and T202 with DB. Furthermore, the electrochemical impedance spectroscopy (EIS) measurements that were conducted showed that there is an upward shift in the  ${}_nE_F$  of the co-sensitized T181-DB and T202-DB devices by  $\sim 40\text{--}50$  mV when compared to the DB device. This shift in the quasi-Fermi energy level in addition to the increase in the charge transfer resistance in the co-sensitized cells are attributed to the increase in the total dye coverage in these cells when compared to the individual ones. As a last conclusion, the method of co-sensitizing of pyridyl-based dyes with carboxylic acid-based dyes proved to be a very successful strategy to increase, light absorption and decrease recombination losses in cobalt-based DSSCs and thus raising the DSSC power conversion efficiency.

## ASSOCIATED CONTENT

### Supporting Information

The Supporting Information is available free of charge on the ACS Publications website at DOI: 10.1021/acsaem.8b00448.

Synthetic schemes, electrochemistry, and absorption spectra of desorbed titania films (PDF)

## AUTHOR INFORMATION

### Corresponding Author

\*E-mail: tarek.ghaddar@aub.edu.lb.

### ORCID

Tarek H. Ghaddar: 0000-0002-7748-0597

### Notes

The authors declare no competing financial interest.

## ACKNOWLEDGMENTS

This work was supported by the University Research Board (Grant 103367) at the American University of Beirut (AUB), the Kamal Shair Research Grant (Grant 103365) at AUB, and the Lebanese National Council for Scientific Research (Grant 103487).

## REFERENCES

- (1) O'Regan, B.; Grätzel, M. A Low-Cost, High-Efficiency Solar Cell Based on Dye-Sensitized Colloidal TiO<sub>2</sub> Films. *Nature* **1991**, *353*, 737–740.
- (2) Kakiage, K.; Aoyama, Y.; Yano, T.; Oya, K.; Fujisawa, J.-i.; Hanaya, M. Highly-Efficient Dye-Sensitized Solar Cells with Collaborative Sensitization by Silyl-Anchor and Carboxy-Anchor Dyes. *Chem. Commun.* **2015**, *51*, 15894–15897.
- (3) Yella, A.; Lee, H.-W.; Tsao, H. N.; Yi, C.; Chandiran, A. K.; Nazeeruddin, M. K.; Diau, E. W.-G.; Yeh, C.-Y.; Zakeeruddin, S. M.; Grätzel, M. Porphyrin-Sensitized Solar Cells with Cobalt (II/III)-Based Redox Electrolyte Exceed 12% Efficiency. *Science* **2011**, *334*, 629–634.
- (4) Mathew, S.; Yella, A.; Gao, P.; Humphry-Baker, R.; Curchod, B. F. E.; Ashari-Astani, N.; Tavernelli, I.; Rothlisberger, U.; Nazeeruddin, M. K.; Grätzel, M. Dye-Sensitized Solar Cells with 13% Efficiency Achieved through the Molecular Engineering of Porphyrin Sensitizers. *Nat. Chem.* **2014**, *6*, 242.
- (5) Yun, M. J.; Cha, S. I.; Seo, S. H.; Kim, H. S.; Lee, D. Y. Insertion of Dye-Sensitized Solar Cells in Textiles Using a Conventional Weaving Process. *Sci. Rep.* **2015**, *5*, 11022.
- (6) Freitag, M.; Teuscher, J.; Saygili, Y.; Zhang, X.; Giordano, F.; Liska, P.; Hua, J.; Zakeeruddin, S. M.; Moser, J.-E.; Grätzel, M.; Hagfeldt, A. Dye-Sensitized Solar Cells for Efficient Power Generation under Ambient Lighting. *Nat. Photonics* **2017**, *11*, 372.
- (7) Tsai, M.-C.; Wang, C.-L.; Chang, C.-W.; Hsu, C.-W.; Hsiao, Y.-H.; Liu, C.-L.; Wang, C.-C.; Lin, S.-Y.; Lin, C.-Y. A Large, Ultra-black, Efficient and Cost-Effective Dye-Sensitized Solar Module Approaching 12% Overall Efficiency under 1000 Lux Indoor Light. *J. Mater. Chem. A* **2018**, *6*, 1995–2003.
- (8) Kuang, D.; Walter, P.; Nüesch, F.; Kim, S.; Ko, J.; Comte, P.; Zakeeruddin, S. M.; Nazeeruddin, M. K.; Grätzel, M. Co-Sensitization of Organic Dyes for Efficient Ionic Liquid Electrolyte-Based Dye-Sensitized Solar Cells. *Langmuir* **2007**, *23*, 10906–10909.
- (9) Hao, Y.; Saygili, Y.; Cong, J.; Eriksson, A.; Yang, W.; Zhang, J.; Polanski, E.; Nonomura, K.; Zakeeruddin, S. M.; Grätzel, M.; Hagfeldt, A.; Boschloo, G. Novel Blue Organic Dye for Dye-Sensitized Solar Cells Achieving High Efficiency in Cobalt-Based Electrolytes and by Co-Sensitization. *ACS Appl. Mater. Interfaces* **2016**, *8*, 32797–32804.
- (10) Islam, A.; Akhtaruzzaman, M.; Chowdhury, T. H.; Qin, C.; Han, L.; Bedja, I. M.; Stalder, R.; Schanze, K. S.; Reynolds, J. R. Enhanced Photovoltaic Performances of Dye-Sensitized Solar Cells by Co-Sensitization of Benzothiadiazole and Squaraine-Based Dyes. *ACS Appl. Mater. Interfaces* **2016**, *8*, 4616–4623.
- (11) Lodermeier, F.; Costa, R. D.; Malig, J.; Jux, N.; Guldi, D. M. Benzoporphyrins: Selective Co-Sensitization in Dye-Sensitized Solar Cells. *Chem. - Eur. J.* **2016**, *22*, 7851–7855.
- (12) Zhang, L.; Cole, J. M. Anchoring Groups for Dye-Sensitized Solar Cells. *ACS Appl. Mater. Interfaces* **2015**, *7*, 3427–3455.
- (13) Harima, Y.; Fujita, T.; Kano, Y.; Imae, I.; Komaguchi, K.; Ooyama, Y.; Ohshita, J. Lewis-Acid Sites of TiO<sub>2</sub> Surface for Adsorption of Organic Dye Having Pyridyl Group as Anchoring Unit. *J. Phys. Chem. C* **2013**, *117*, 16364–16370.
- (14) Stergiopoulos, T.; Rozi, E.; Karagianni, C.-S.; Falaras, P. Influence of Electrolyte Co-Additives on the Performance of Dye-Sensitized Solar Cells. *Nanoscale Res. Lett.* **2011**, *6*, 307–307.
- (15) Yum, J.-H.; Jang, S.-R.; Walter, P.; Geiger, T.; Nüesch, F.; Kim, S.; Ko, J.; Grätzel, M.; Nazeeruddin, M. K. Efficient Co-Sensitization of Nanocrystalline TiO<sub>2</sub> Films by Organic Sensitizers. *Chem. Commun.* **2007**, 4680–4682.
- (16) Ooyama, Y.; Inoue, S.; Nagano, T.; Kushimoto, K.; Ohshita, J.; Imae, I.; Komaguchi, K.; Harima, Y. Dye-Sensitized Solar Cells Based on Donor–Acceptor  $\Pi$ -Conjugated Fluorescent Dyes with a Pyridine Ring as an Electron-Withdrawing Anchoring Group. *Angew. Chem.* **2011**, *123*, 7567–7571.
- (17) Ooyama, Y.; Nagano, T.; Inoue, S.; Imae, I.; Komaguchi, K.; Ohshita, J.; Harima, Y. Dye-Sensitized Solar Cells Based on Donor- $\Pi$ -Acceptor Fluorescent Dyes with a Pyridine Ring as an Electron-Withdrawing-Injecting Anchoring Group. *Chem. - Eur. J.* **2011**, *17*, 14837–14843.
- (18) Shibayama, N.; Ozawa, H.; Ooyama, Y.; Arakawa, H. Highly Efficient Cosensitized Plastic-Substrate Dye-Sensitized Solar Cells with Black Dye and Pyridine-Anchor Organic Dye. *Bull. Chem. Soc. Jpn.* **2015**, *88*, 366–374.
- (19) Shibayama, N.; Ozawa, H.; Abe, M.; Ooyama, Y.; Arakawa, H. A New Cosensitization Method Using the Lewis Acid Sites of a TiO<sub>2</sub> Photoelectrode for Dye-Sensitized Solar Cells. *Chem. Commun.* **2014**, *50*, 6398–6401.
- (20) Ellis, H.; Eriksson, S. K.; Feldt, S. M.; Gabriellsson, E.; Lohse, P. W.; Lindblad, R.; Sun, L.; Rensmo, H. k.; Boschloo, G.; Hagfeldt, A. Linker Unit Modification of Triphenylamine-Based Organic Dyes for Efficient Cobalt Mediated Dye-Sensitized Solar Cells. *J. Phys. Chem. C* **2013**, *117*, 21029–21036.
- (21) Bai, Y.; Zhang, J.; Zhou, D.; Wang, Y.; Zhang, M.; Wang, P. Engineering Organic Sensitizers for Iodine-Free Dye-Sensitized Solar Cells: Red-Shifted Current Response Concomitant with Attenuated Charge Recombination. *J. Am. Chem. Soc.* **2011**, *133*, 11442–11445.
- (22) Jeon, Y.; Kim, T.-M.; Kim, J.-J.; Hong, J.-I. Vacuum-Depositible Thiophene-and Benzothiadiazole-Based Donor Materials for Organic Solar Cells. *New J. Chem.* **2015**, *39*, 9591–9595.
- (23) Frisch, M. J.; Trucks, G. W.; Schlegel, H. B.; Scuseria, G. E.; Robb, M. A.; Cheeseman, J. R.; Montgomery, J. A., Jr.; Vreven, T.; Kudin, K. N.; Burant, J. C.; Millam, J. M.; Iyengar, S. S.; Tomasi, J.; Barone, V.; Mennucci, B.; Cossi, M.; Scalmani, G.; Rega, N.; Petersson, G. A.; Nakatsuji, H.; Hada, M.; Ehara, M.; Toyota, K.; Fukuda, R.; Hasegawa, J.; Ishida, M.; Nakajima, T.; Honda, Y.; Kitao, O.; Nakai, H.; Klene, M.; Li, X.; Knox, J. E.; Hratchian, H. P.; Cross, J. B.; Adamo, C.; Jaramillo, J.; Gomperts, R.; Stratmann, R. E.; Yazyev, O.; Austin, A. J.; Cammi, R.; Pomelli, C.; Ochterski, J. W.; Ayala, P. Y.; Morokuma, K.; Voth, G. A.; Salvador, P.; Dannenberg, J. J.; Zakrzewski, V. G.; Dapprich, S.; Daniels, A. D.; Strain, M. C.; Farkas, O.; Malick, D. K.; Rabuck, A. D.; Raghavachari, K.; Foresman, J. B.; Ortiz, J. V.; Cui, Q.; Baboul, A. G.; Clifford, S.; Cioslowski, J.; Stefanov, B. B.; Liu, G.; Liashenko, A.; Piskorz, P.; Komaromi, I.; Martin, R. L.; Fox, D. J.; Keith, T.; Al-Laham, M. A.; Peng, C. Y.; Nanayakkara, A.; Challacombe, M.; Gill, P. M. W.; Johnson, B.; Chen, W.; Wong, M. W.; Gonzalez, C.; Pople, J. A., *Gaussian 03*; Gaussian: Pittsburgh, PA, USA, 2003.
- (24) Cossi, M.; Barone, V. *J. Chem. Phys.* **2001**, *115*, 4708–4717.
- (25) Jiang, X.; Karlsson, K. M.; Gabriellsson, E.; Johansson, E. M. J.; Quintana, M.; Karlsson, M.; Sun, L.; Boschloo, G.; Hagfeldt, A. Highly Efficient Solid-State Dye-Sensitized Solar Cells Based on Triphenylamine Dyes. *Adv. Funct. Mater.* **2011**, *21*, 2944–2952.
- (26) Su, J.; Zhu, S.; Chen, R.; An, Z.; Chen, X.; Chen, P. Study on Dye-Loading Mode on TiO<sub>2</sub> Films and Impact of Co-Sensitizers on

Highly Efficient Co-Sensitized Solar Cells. *J. Mater. Sci.: Mater. Electron.* **2017**, *28*, 3962–3969.

(27) Aung, S. H.; Hao, Y.; Oo, T. Z.; Boschloo, G. 2-(4-Butoxyphenyl)-N-Hydroxyacetamide: An Efficient Preadsorber for Dye-Sensitized Solar Cells. *ACS Omega* **2017**, *2*, 1820–1825.

(28) González-Pedro, V.; Xu, X.; Mora-Seró, I.; Bisquert, J. Modeling High-Efficiency Quantum Dot Sensitized Solar Cells. *ACS Nano* **2010**, *4*, 5783–5790.

(29) Guillén, E.; Peter, L. M.; Anta, J. A. Electron Transport and Recombination in ZnO-Based Dye-Sensitized Solar Cells. *J. Phys. Chem. C* **2011**, *115*, 22622–22632.

(30) Rühle, S.; Greenshtein, M.; Chen, S. G.; Merson, A.; Pizem, H.; Sukenik, C. S.; Cahen, D.; Zaban, A. Molecular Adjustment of the Electronic Properties of Nanoporous Electrodes in Dye-Sensitized Solar Cells. *J. Phys. Chem. B* **2005**, *109*, 18907–18913.

(31) Bisquert, J.; Cahen, D.; Hodes, G.; Rühle, S.; Zaban, A. Physical Chemical Principles of Photovoltaic Conversion with Nanoparticulate, Mesoporous Dye-Sensitized Solar Cells. *J. Phys. Chem. B* **2004**, *108*, 8106–8118.

(32) Cahen, D.; Hodes, G.; Grätzel, M.; Guillemoles, J. F.; Riess, I. Nature of Photovoltaic Action in Dye-Sensitized Solar Cells. *J. Phys. Chem. B* **2000**, *104*, 2053–2059.

(33) Pazoki, M.; Lohse, P. W.; Taghavinia, N.; Hagfeldt, A.; Boschloo, G. The Effect of Dye Coverage on the Performance of Dye-Sensitized Solar Cells with a Cobalt-Based Electrolyte. *Phys. Chem. Chem. Phys.* **2014**, *16*, 8503–8508.